Control Engineering Practice 56 (2016) 101–110

Contents lists available at ScienceDirect

Control Engineering Practice

journal homepage: www.elsevier.com/locate/conengprac

Virtual shaft: Synchronized motion control for real time testing of automotive powertrains

J. Andert [a,*], S. Klein [a], R. Savelsberg [b], S. Pischinger [b], K. Hameyer [c]

[a] Junior Professorship for Mechatronic Systems for Combustion Engines, RWTH Aachen University, Forckenbeckstraße 4, 52074 Aachen, Germany
[b] Institute for Combustion Engines, RWTH Aachen University, Forckenbeckstraße 4, 52074 Aachen, Germany
[c] Institute of Electrical Machines, RWTH Aachen University, Schinkelstraße 4, 52062 Aachen, Germany

ARTICLE INFO

Article history:
Received 12 October 2015
Received in revised form
11 August 2016
Accepted 12 August 2016

Keywords:
Synchronized motion control
Virtual shaft
Cascaded controllers
Power train testing
Engine and transmission test bench

ABSTRACT

The complexity of automobile powertrains continues to rise, leading to increased development time and effort. Synchronous testing with spatially distributed test benches allows improvements by front-loading of the validation phase. Nevertheless, virtualization of the mechanical interaction of shaft connections is required. A virtual shaft algorithm (VSA) is investigated for synchronized motion control in separate test benches. The behavior of a rigid mechanical shaft is analyzed and modeled. The mechanical shaft is substituted by two electrical motors and a superimposed VSA controller. This virtual shaft is established between two test benches for a combustion engine and a mechanical transmission. Control algorithms for synchronized motion control, known from web machines and force feedback, are analyzed. A controller layout with separate torque and speed controllers is implemented and analyzed through transfer function mathematics. The controllers are parametrized analytically for different gears. The effect of communication delay on the VSA is analyzed by simulation. The open clutch situation is handled by deactivation of the torque feedback. Validation on real test benches shows small deviations for torque and speed. Further work will focus on the necessity of system knowledge for controller layout and on the transient behavior during shifting.

1. Introduction

The rising number and complexity of components in modern powertrains has led to significant efforts in development and testing. Virtualization allows one to shift tasks to earlier project phases (front-loading) by utilizing specialized test benches instead of prototype vehicles (road to rig) (Dodds & Plummer, 2001; List & Schoeggl; Pelkmans & Debal, 2006; Sciuto & Hellmund, 2001), thereby enabling the test procedure on the road to be replaced by a test bench with simulated vehicle and road components. During development, each element of the powertrain is analyzed separately by considering component-specific requirements. Combustion engine test benches offer excellent possibilities for emission and efficiency analysis. Transmission test benches are focused on durability tests and noise, vibration and harshness analysis. Powerful electric motors can be used to simulate the high torques at the vehicle's wheels.

In Andert & Savelsberg (2015) and Andert, Huth, Savelsberg & Politsch (2015), the road-to-rig idea is explored and extended by connecting multiple test objects to a cyber-physical system with a virtualized mechanical shaft connection. The aim of this approach is to couple component test facilities to a virtual powertrain test bench with a superordinated control logic that emulates a mechanical shaft connection (Fig. 1).

Each of the testing facilities consists of a controlled electric load machine at the open end of the test object. The superimposed controller synchronizes speed and torque in a way that corresponds to a rigid shaft connection with low inertia and high stiffness.

The synchronization of multi-motor systems to substitute mechanical shafts is implemented in most industrial web machines and the theoretical background is well known in control theory (Anderson, Meyer, Valenzuela, & Lorenz; Liu, Li, & Zhang, 2012; Lorenz & Schmidt; Payette, 1998, 1999; Sun, 2003; Tomizuka, Hu, Chiu, & Kamano, 1992). A good survey for the past 20 years is given by Pérez-Pinal, Nuñez, Álvarez, and Cervantes. However, in all investigated approaches and realizations derived from industrial

* Corresponding author.
E-mail addresses: andert@vka.rwth-aachen.de (J. Andert), klein_se@vka.rwth-aachen.de (S. Klein), savelsberg@vka.rwth-aachen.de (R. Savelsberg), pischinger_s@vka.rwth-aachen.de (S. Pischinger), kay.hamayer@iem.rwth-aachen.de (K. Hameyer).

http://dx.doi.org/10.1016/j.conengprac.2016.08.005
0967-0661/

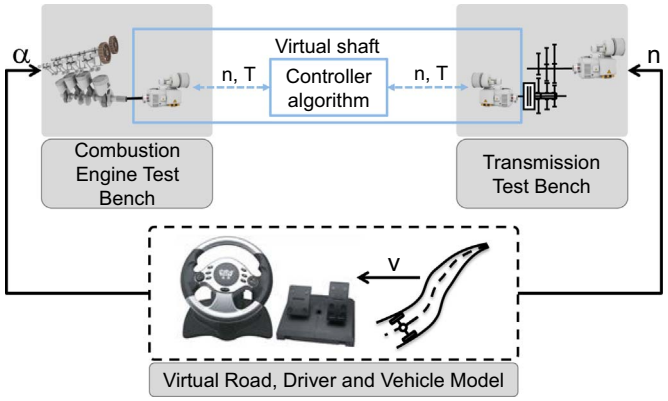

Fig. 1. New testing approach employing synchronized motion control emulating a mechanical shaft (Andert & Savelsberg, 2015).

application, the speed and partially the angular position are controlled. For a substitution of the mechanical shaft in automotive powertrain testing, the torque must be synchronized as well; this is not covered by state-of-the-art approaches.

A more similar technical realization is the steer-by-wire approach with force feedback. In conventional steering systems, the steering wheel is mechanically connected to the front wheels. In the steer-by-wire approach, one substitutes this connection with a steering motor and a feedback motor, both of which are electric motors. In the past few decades steer by wire has attracted particular attention (Bertoluzzo, Buja, & Menis, 2007; Kenned & Patil; Wang et al., 2014). In most approaches, the measured and processed steering wheel angle defines the set point of the front wheels and the measured wheel torque is superimposed on the steering wheel torque applied by the driver to get realistic steering feedback.

This control structure represents a kind of a coupled system and seems to be very similar to the virtual shaft setup proposed in this paper. However, the requirements and the problems differ here. The master and slave topology of steer by wire has two operating directions. The steering wheel position is used as an externally defined set point, and the reaction force is fed back with a low gain to the driver. Because power-assisted steering is required, feedback torque and mechanical power at the feedback motor are significantly lower in comparison to the wheel actuator. Owing to the constrained torque feedback and the stabilizing driver behavior, instability and oscillations can be avoided and the system can be considered as two separate single-input and single-output systems (Amberkar, Bolourchi, Demerly, & Millsap).

In contrast, coupling in the virtual shaft algorithm (VSA) is identical in both operation directions with the same priority. The resulting system interactions and the effects on controller layout will be discussed in this paper.

2. Theory

2.1. System model

The first step in substituting a real mechanical shaft by a virtual shaft connection is the understanding and the mathematical description of its behavior. A simple model for a physical shaft, in which torsion, stiffness, and distortion are neglected, is an inertia with two applied torques at each end of the shaft. A measurement point divides the moment of inertia into two subinertia (Fig. 2). Under these considerations, the physical description of the measured torque can be written in two ways:

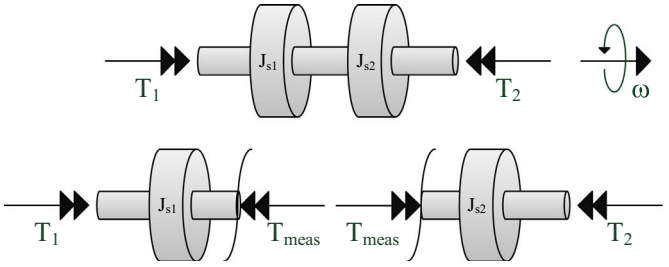

Fig. 2. Ideal mechanical shaft with torque measurement.

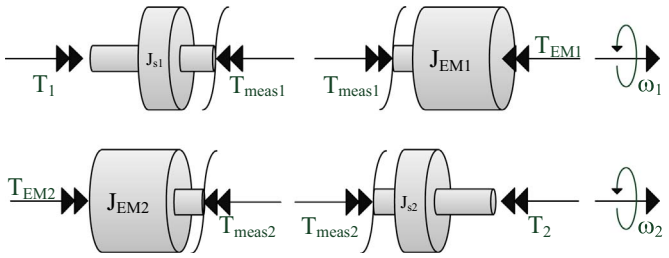

Fig. 3. Divided virtual shaft with ideal internal torque sources and inertias.

$$T_{meas} = T_1 - J_{s1}\cdot\dot{\omega},\ T_{meas} = J_{s2}\cdot\dot{\omega} + T_2. \tag{1}$$

Elimination of $\dot{\omega}$ in Eq. (1) and conversion in terms of T_{meas} leads to

$$T_{meas} = \frac{T_1 J_{s2} + T_2 J_{s1}}{J_{s1} + J_{s2}}. \tag{2}$$

The rotational speed ω can be described depending on two out of three shaft torques $T_{1/2}$ and T_{meas}, accordingly:

$$\omega = \int_{-\infty}^{t} \frac{T_1 - T_{meas}}{J_{s1}} dt = \int_{-\infty}^{t} \frac{T_{meas} - T_2}{J_{s2}} dt = \int_{-\infty}^{t} \frac{T_1 - T_2}{J_{s1} + J_{s2}} dt. \tag{3}$$

Eqs. (1)–(3) will be used to describe the reduced physical behavior of a shaft with reference to a measurement point.

A separation of the ideal shaft into two systems without a mechanical connection is then conducted (Fig. 3). The respective open end is connected to an electric motor that simulates the mechanical shaft connection. The inertias $J_{s1/2}$ describe the inertia of the divided ideal shaft as shown previously in Fig. 2. Both electric motors are represented by torque sources $T_{1/2}$. The additional inertia of the electric machine cannot be neglected and is represented by $J_{EM1/2}$.

The target of the VSA is to control the divided systems in a way that corresponds to the reference layout (see Fig. 2). Eq. (4) shall be fulfilled at any time. If this requirement is fulfilled, the separate systems interact exactly like the reference system and any influence of the inertia $J_{EM1,2}$ is compensated implicitly.

$$T_{meas1} \stackrel{!}{=} T_{meas2} \stackrel{!}{=} T_{meas}\omega_1 \stackrel{!}{=} \omega_2 \stackrel{!}{=} \omega \tag{4}$$

According to the proposed structure and with Eqs. (1)–(3), the torque and speed of both systems is described by

$$T_{meas1} = \frac{T_1 J_{EM1} + T_{EM1} J_{s1}}{J_{EM1} + J_{s1}},\ T_{meas2} = \frac{T_{EM2} J_{s2} + T_2 J_{EM2}}{J_{EM2} + J_{s2}},$$
$$\omega_1 = \int_{-\infty}^{t} \frac{T_1 - T_{meas1}}{J_{s1}} dt,\ \omega_2 = \int_{-\infty}^{t} \frac{T_{meas2} - T_2}{J_{s2}} dt, \tag{5}$$

with

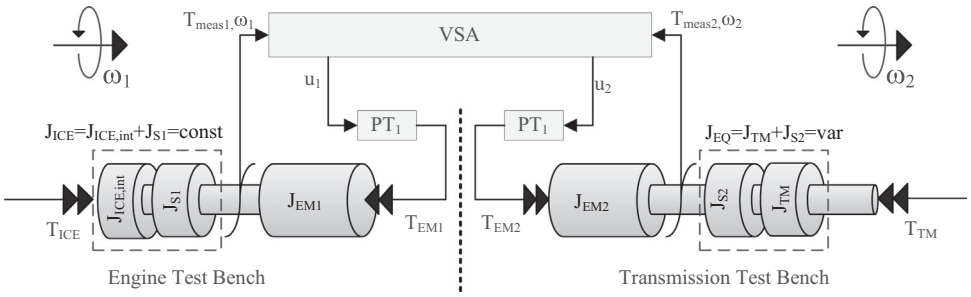

Fig. 4. VSA applied to engine and transmission test bench.

$T_{1/2}$ = torque applied externally,

$T_{meas1/2}$ = measured torque,

$J_{EM1/2}$ = inertia of electric motor, and $J_{s1/s2}$ = shaft inertia.

The electric motors are defined as control outputs of the VSA. The dynamic behavior of a torque- or speed-controlled electric motor can be described by a dead time representing the communication and inverter delay and at least one first-order lag for the control lag (Schröder, 2009). In this study, a dead-time transfer function in combination with a PT_1 is supposed:

$$G_{EM}(s) = K_{EM}\frac{e^{-sT_{EM,t}}}{T_{EM}s + 1}. \tag{6}$$

Based on these assumptions, the divided shaft (Fig. 3) is applied to a spatially distributed automotive powertrain. The internal combustion engine (ICE) and the transmission (TM) are located in two different test benches. The virtual shaft is applied between the crankshaft of the ICE and the clutch input of the transmission (Fig. 4). The ICE is modeled as an ideal internal torque source T_{ICE} and a constant inner inertia $J_{ICE,int}$ that corresponds to all rotating parts. $J_{ICE,int}$ and J_{s1} have the same rotation speed and can be combined as J_{ICE}. The same approach is used for J_{TM}, representing transmission, clutch, final drive, and vehicle inertia. Naturally, the equivalent inertia of the transmission test bench, J_{EQ}, depends on the engaged gear and on the status of the clutch (open or closed). In particular, in an open-clutch situation, J_{EQ} reaches very low values.

The VSA controls both electric machines with a PT_1 behavior as described before. The set point of the electric machine in the ICE test bench, u_1, is influenced by the output u_2 and vice versa. Therefore, the systems are strongly coupled. In the next section, a cascaded control based on a force-feedback approach is designed to solve this issue. For the sake of simplicity the dead time will be neglected in the next section, but afterwards it will be included in the simulation.

2.2. Controller structure

A torque and speed synchronization approach corresponding to a steer-by-wire system is applied. In Amberkar et al., two separate torque and position feedback loops are proposed. This concept is transferred to control the speed in the ICE bench and the torque in the transmission bench. This definition is according to a conventional testing procedure but could also be applied vice versa. The synchronization point is achieved if each set point matches the measured value of the other system and the closed loop is strictly stable. Hence, both feedback loops have the same priority and no master/slave topology is applicable as used in conventional steer-by-wire applications.

Owing to their simple implementation and wide use, in a first approach PID controllers are implemented. The torque and speed controller outputs are described in the frequency domain by

$$u(t) = 0 \;\forall\; t < 0, \tag{7}$$

$$u_1 = (\omega_1 - \omega_2)\cdot G_{PID1} \tag{8}$$

$$u_2 = (T_{meas,2} - T_{meas,1})\cdot G_{PID2}. \tag{9}$$

PID_1 controls the speed of the electric load machine of the combustion engine according to the set point measured at the transmission input and PID_2 controls the torque of the transmission input, respectively.

This interpretation shows clearly the coupling of both systems and the dependencies of the two controllers. In other words, the first PID controller is part of the second loop and must be considered during the parameterization of the second controller and vice versa. Any decoupling algorithms such as those in Boksenbom & Hood, Luyben (1970), and Föllinger & Konigorski (2013) are not applicable, because the synchronization would be lost.

The intended coupling of the systems, which can be seen as a target of the VSA, is the main issue during the parameterization of the PID controllers. The resulting control structure under consideration of the coupling is shown in Fig. 5.

This structure is similar to a cascaded control with the transmission bench as the inner loop (torque feedback) and the engine bench as the outer loop (speed feedback). The transmission input torque T_{TM} and the engine torque T_{ICE} are interpreted as disturbances and will be neglected for the controller layout. The open-loop transfer function of the inner loop corresponds to a first-order lag with an inertia-dependent gain:

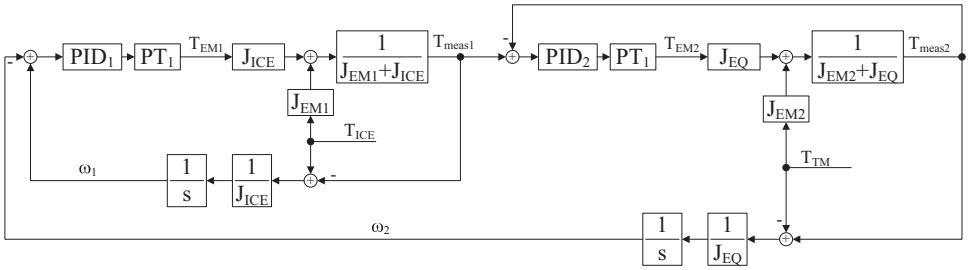

Fig. 5. VSA structure with two cascaded PID controllers.

Table 1
Powertrain configuration.

Parameter	Value
$m_{Vehicle}$	1320 kg
J_{ICE}	0.213 kg m^2
J_{EM1}	0.85 kg m^2
J_{EM2}	0.072 kg m^2
J_s	0.0001 kg m^2
T_{EM1}	0.032 s
T_{EM2}	0.025 s
i_{Gear1}	3.83
i_{Gear2}	2.2
i_{Gear3}	1.4
i_{Gear4}	1
i_{Gear5}	0.81
$i_{FinalDrive}$	3.743

Table 2
Inertia/gain dependency of selected gear for a system without dead time.

Gear	J_{EQ} (kg m^2)	G_{PID1}	G_{PID2}
N	0.0001	$T_I = 0.0762$ $T_D = 0.019$ $K_p = 1.76$	$T_I = 0.012$ $T_D = 2{\cdot}10^{-4}$ $K_P = 1.5{\cdot}10^4$
1–5		$T_I = 0.4052$ $T_D = 0.0411$	$T_I = 0.0047$ $T_D = 4{\cdot}10^{-6}$
1	0.639	$K_P = 69.7$	$K_P = 4.26$
2	1.937	$K_P = 211$	$K_P = 3.97$
3	4.783	$K_P = 521$	$K_P = 3.89$
4	9.374	$K_P = 1020$	$K_P = 3.86$
5	14.278	$K_P = 1560$	$K_P = 3.85$

$$G_{o,TM}(s) = G_{PID2}(s)\cdot\frac{K_{EM2}}{T_{E2}s+1}\cdot\frac{J_{EQ}}{J_{EM2}+J_{EQ}}. \tag{10}$$

The reference transfer function can be described as

$$G_{w,TM}(s) = \frac{G_{PID2}(s)}{\frac{T_{E2}}{K_{w2}}s + \frac{1}{K_{w2}} + G_{PID2}(s)},\ K_{w2} = K_{EM2}\cdot\frac{J_{EQ}}{J_{EM2}+J_{EQ}}. \tag{11}$$

The inner closed-loop transfer function $G_{w,TM}(s)$ depends on the system inertias J_{EM2} and J_{EQ}. As the equivalent inertia J_{EQ} depends on the engaged gear and the clutch situation, the tuning of the PID factors has to be performed for each system state separately.

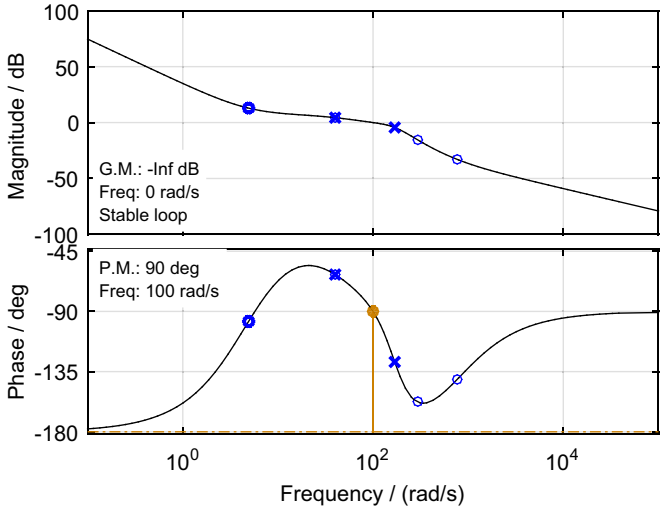

Fig. 6. Bode diagram outer open loop for all gears.

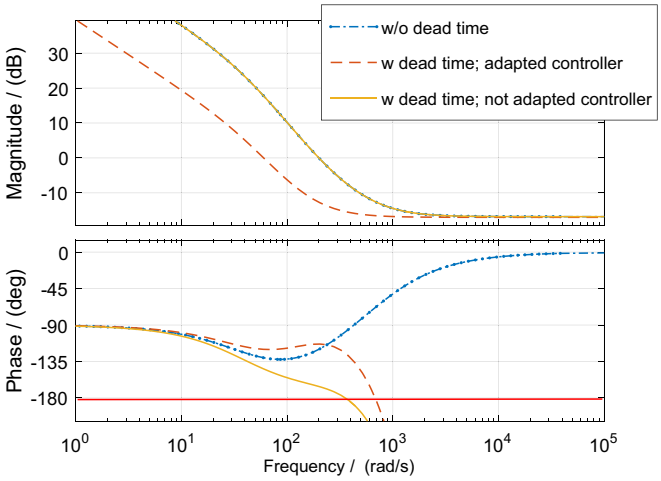

Fig. 7. Bode diagram inner open loop with and without dead time.

The inner reference transfer function $G_{w,TM_\omega}(s)$ related to the transmission speed can be written as

$$G_{w,TM_\omega}(s) = G_{w,TM}(s)\cdot\frac{1}{J_{EQ}s}. \tag{12}$$

For the estimation of the open-loop transfer function of the outer loop (speed feedback), Eq. (12) has to be taken into account:

$$G_{o,ICE}(s) = G_{PID1}(s)\cdot\frac{K_{EM1}}{T_{E1}s+1}\cdot\frac{J_{ICE}}{J_{EM1}+J_{ICE}}\cdot G_{w,TM_\omega}(s). \tag{13}$$

The derived functions show a structure similar to a cascade. To utilize this analogy, ω_2 is defined as the control variable and ω_1 as an external setpoint. In other words PID_1 controls indirectly the speed of the transmission test bench. However the definition of ω_1 as the set point leads to a model error. An example for the performance impact of the inner loop on the outer loop is shown in Section 2.4.3.

2.3. Controller parametrization

The controller is adapted to a vehicle powertrain with 5 speed manual transmission as listed in Table 1. In the first instance, the PID gains are calibrated for the derived control plants of the ideal system (cp. Eqs. (10) and (13)). Afterwards, dead-time is added to the system and the effects on controller parametrization are analyzed.

2.3.1. System without dead time

PID-design conditions are a phase margin of 60° for the inner loop and 90° for the outer loop. The high margin for the outer loop is chosen to suppress undesired overshoots of the rotational speed. The maximum bandwidth is given by the finite constrains of the

Table 3
Inertia/gain dependency of selected gear for a dead time system.

Gear	J_{EQ} (kg m^2)	G_{PID1}	G_{PID2}
1–5		$T_I = 0.0122$ $T_D = 0.003$	$T_I = 0.0122$ $T_D = 0.003$
1	0.639	$K_P = 148$	$K_P = 1.29$
2	1.937	$K_P = 229$	$K_P = 1.2$
3	4.783	$K_P = 353$	$K_P = 1.18$
4	9.374	$K_P = 461$	$K_P = 1.17$
5	14.278	$K_P = 527$	$K_P = 1.17$

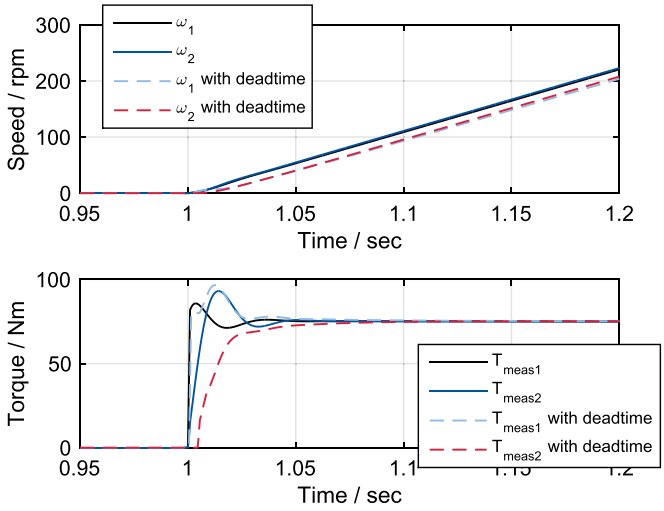

Fig. 8. Step response of virtual shaft with and without dead time for first gear.

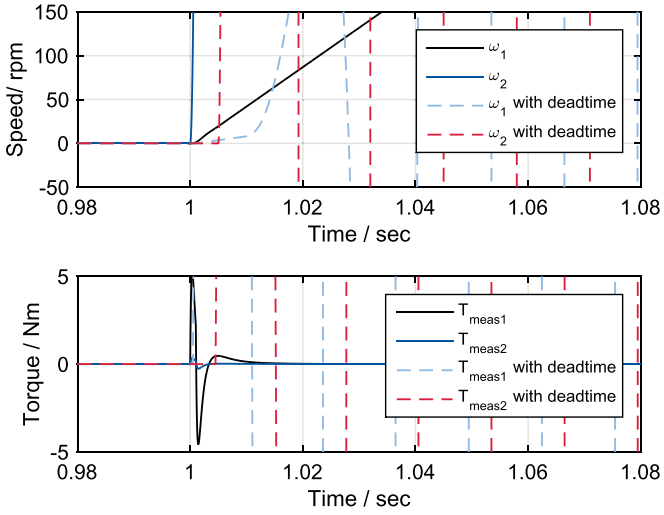

Fig. 9. Unstable VSA step response with dead time for an open clutch.

hardware used for the experiment (e.g. maximum torque gradients). Under these conditions the calibration is done by using bode plot open loop shaping. Tuning of the PID factors is done depending on the clutch state and engaged gear accordingly. The influence of J_{EQ} on the PID factors for both controllers is listed in Table 2.

In gears 1–5 the controller gains are chosen to have exactly the same closed loop behavior. Owing to the same dynamics (locus of poles and zeroes), only the loop gain is adapted to achieve the exact same response. The bode plot of the outer open loop is given in Fig. 6 and represents all engaged gear control plants. With the help of the bode plot it can easily be shown that the phase margin is always greater 0° for all possible closed loop gains. Therefore, from a stability point of view the PID configuration set with the highest gain (here gear 5) would be viable for the other gears. Hardware constraints and hardware protection limit the viable maximum jerk to the crank shaft and the transmission input shaft. Thus an optimal control performance is achieved with constant maximum bandwidth and different sets of PID-controller gains.

As shown in Table 2, the small inertia J_{EQ} in neutral gear results in PID gains that are far higher than in engaged gear situations.

2.3.2. Dead time system

For a more realistic behavior, the model is extended by a communication dead time of 500 µs and an electrical machine inverter dead time of 4 ms. The dead time elements are approximated as second order all-pass filters, obtained by a second order Padé-approximation (Normey-Rico & Camacho, 2007). The open loop transfer functions (Eqs. (10) and (13)) and the PID-controller parameter sets are adapted accordingly. The controller gain for systems with dead time must be decreased to achieve a stable loop (Normey-Rico & Camacho, 2007). Fig. 7 illustrates the adaption for the inner loop with engaged first gear. The dash-dotted curve shows the amplitude and phase response without any dead time. The bandwidth is designed set to 200 rad/s, resulting in a phase margin of 60°. The solid line shows a combination of non-dead time controller and dead time systems resulting in a phase margin of <14°. The dashed line shows the adapted controller according to the dead time system. The phase margin is adjusted to 60°, but the bandwidth is decreased to 60 rad/s.

The controller configuration for the system with dead time is given in Table 3.

A detailed analysis of transient effects and the control quality is done by simulations and subsequent test bench measurements.

2.4. Simulation results

For a first evaluation of the transient behavior, the VSA controller is tested in a simulated environment. A Matlab/Simulink model with a fixed step size of 50 µs is created based on available test bench components. The electric machines are represented by inertia and ideal torque sources with a PT_1 behavior and a speed-dependent torque limit. In general, the PT_1 lag and communication latency are variable and can be adapted to different configurations. The simulation is conducted for engaged gears and an open-clutch situation as listed in Table 2.

2.4.1. Engaged gear situation

The system step response without dead time to a stimulus by torque T_{ICE} is shown in Fig. 8 with solid lines. After a short transient period, both torque and speed signals, $T_{meas1/2}$ and $\omega_{1/2}$, show good congruence. The controller reaction to the input step is stable and no persistent oscillations are observed.

In the dead time simulation the system is stimulated by the same input function and the results are shown as dashed lines in the same Fig. 8. Apparently, the dead time results in a delay at the beginning of the step and consecutively leads to a larger control error. However, the system is still stable and the stationary point of both systems is approximately equivalent.

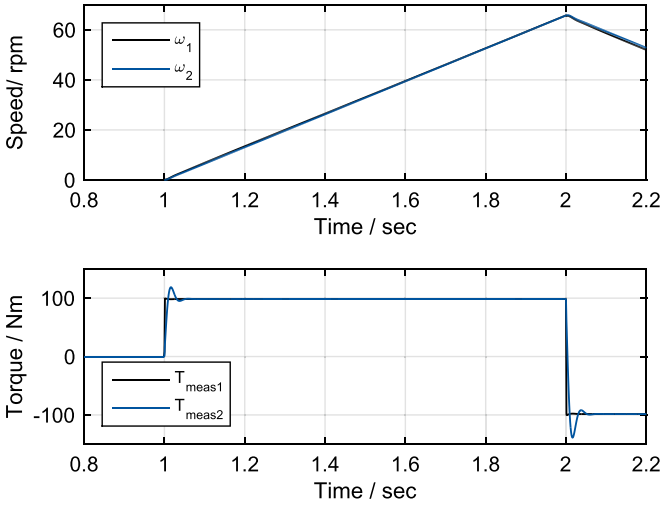

Fig. 10. VSA step response with a correct controller set.

Table 4
Correct parameter set for gear 5.

Controller	Plant
PID_2	TM in gear 5
PID_1	PID_2 for gear 5

Table 5
False parameter set for gear 5.

Controller	Plant
PID_2	TM in gear 5
PID_1	PID_2 for gear 1

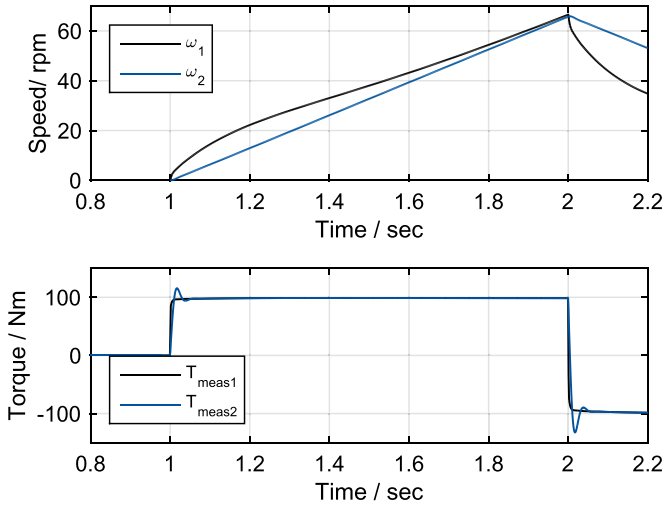

Fig. 11. VSA step response with a wrong controller set.

2.4.2. Open clutch situation

A problem occurs in an open-clutch situation. As described in Section 2.3 the PID gains were adapted for a system with dead time. Nevertheless in neutral gear stable operation cannot be achieved. Fig. 9 shows the unstable VSA step response for a dead time system. Furthermore, the controller gains are not viable in a real experimental setup and an alternative approach is required.

The measured torque of the non-separate reference system can be described by

$$T_{meas} = \frac{T_{ICE} \cdot J_{EQ} - T_{TM} \cdot J_{ICE}}{J_{ICE} + J_{EQ}}. \tag{14}$$

For an open-clutch situation, the input torque T_{TM} is zero. J_{EQ} is dominated by the shaft inertia J_s, which can be neglected in comparison with the combustion engine inertia J_{ICE}. This results in

$$T_{meas,OC} = T_{ICE} \cdot \frac{J_{EQ}}{J_{ICE} + J_{EQ}} \overset{J_{EQ} \ll J_{ICE}}{\rightarrow} 0. \tag{15}$$

In the open-clutch situation, no torque feedback will occur and the cascaded controller structure is no longer required. Instead, only the speed signals $\omega_{1/2}$ have to be synchronized. The reference system has a high inertia J_{ICE} on the combustion engine side and a low inertia J_s on the transmission side. Plausibility considerations indicate that the engine speed should be used as the reference signal and the transmission input speed should follow.

Therefore, a fundamental change of the controller structure is required for the open-clutch situation in a system with

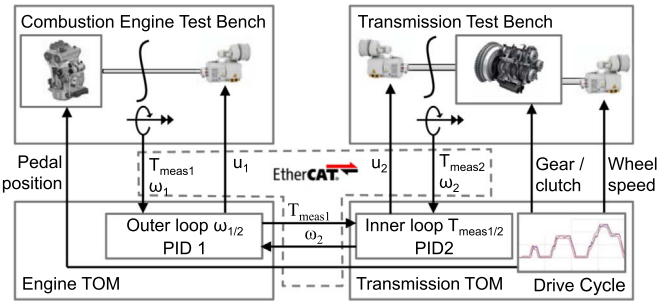

Fig. 12. Implementation of VSA on spatially distributed test benches and TOM systems.

communication latencies. The speed controller PID_1 of the ICE side is deactivated. The torque controller PID_2 of the transmission will change to a speed control manner to follow the ICE speed without a torque feedback signal. Because the shaft inertia is low in comparison with the electric motor inertia, PID parametrization is done according to an open-load situation.

The simulation shows that the system behavior is strongly dependent on communication latencies. A stable controller parametrization cannot be achieved for an open-clutch situation and a change of the controller structure is required. Detection of this situation by a clutch actuator position sensor has to be implemented to ensure component safety during testing.

2.4.3. Controller dependency

As shown in Eq. (13), the transfer functions of the engine testbench speed controller PID_1 depends on the reference transfer function of the transmission test and the equivalent inertia J_{EQ}. The reciprocal dependencies were taken into account during controller parametrization. Simulations are carried out to analyze the sensitivity of this approach. A well-tuned system according to the proposed VSA is compared to an estimated wrong gear.

Fig. 10 shows the response of the non-dead time system to a stimulus by torque T_{ICE}. The 5th gear is engaged and the clutch is closed. The controller gains are parametrized according to the scheme developed in this study. G_{PID1} is calculated under consideration of the correct inner loop including G_{PID2} (cp. Table 4).

A good torque and speed synchronization is achieved and the coupled system is stable.

In a next step, a mismatched parametrization is investigated. The outer loop controller is computed based on a wrong inner loop, in this case for gear 1 instead of gear 5 (cp. Table 5).

The results shown in Fig. 11 demonstrate the impact of the transmission test bench on the ICE test bench controller. The torque signals still show good congruency, but the speed control quality is clearly deteriorated (Fig. 11). The torque set point is determined correctly and the outer controller has to limit the speed of the ICE test bench. The supposed inertia is too low, therefore the braking torque is too low and the speed of the ICE is overshooting.

Table 6
Characteristics of the internal combustion engine.

Cylinder number	6
Displacement	2.5 l
Nominal power	110 kW
Nominal torque	215 N m

Table 7
Characteristics of the electric motor used for the VSA.

Parameter (unit)	EM_1, ATS ASM	EM_2, K&A PMSM
M (N m)	343	90
n (min^{-1})	5000	6400
U (V)	460	405
I (A)	304	408
J (kg m^2)	0.85	0.072

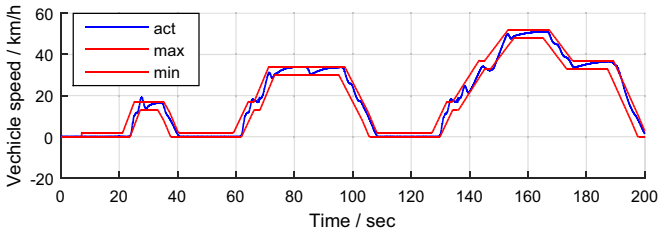

Fig. 13. Result of VSA test procedure, speed boundaries according to ECE-15.

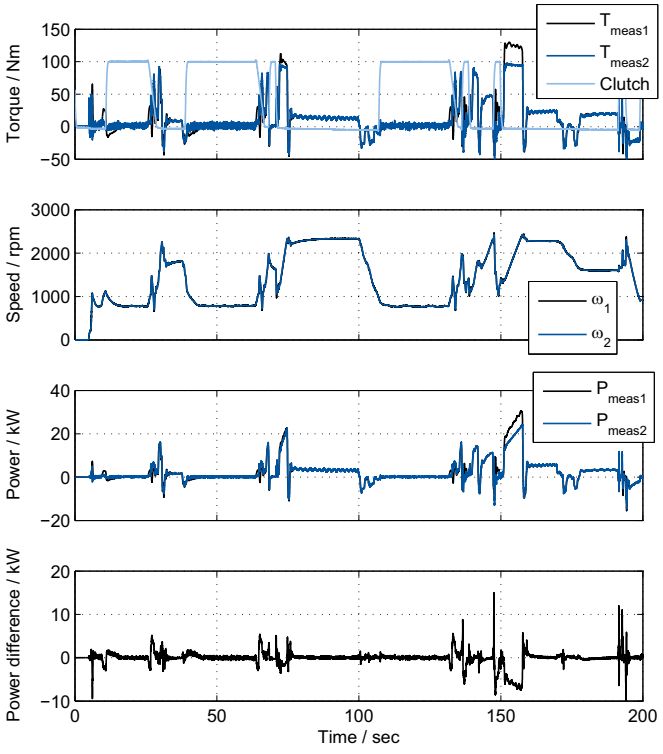

Fig. 14. Torque/speed profiles of ICE and transmission in ECE test cycle.

3. Experimental setup

At the Center for Mobile Propulsion of RWTH Aachen University, different test benches for combustion engines, heavy duty engines, range extenders, transmissions, batteries, and electric machines are available. This infrastructure allows a flexible configuration of hybrid and conventional power-trains with virtualized interaction. A combustion engine and a separated transmission test bench are used to implement and test the VSA.

The simulation results indicated a strong correlation of controller stability and communication latency. Therefore, strictly deterministic communication behavior is a requirement to ensure component safety. Cena, Bertolotti, Scanzio, Valenzano, and Zunino (2012) show that the EtherCAT communication protocol with a distributed clock mechanism can meet hard real-time constraints. This approach is used for the communication between both test benches, the respective frequency inverters, and torque measurement devices. Both test benches are managed by an FEV Test Object Manager (TOM). The VSA is implemented as a distributed system with PID_1 and PID_2 located on different TOM systems and synchronized by the distributed clock algorithm. The desired control trajectory of engine load and gear position is derived from the drive cycle and directly controlled by the transmission TOM system (Fig. 12).

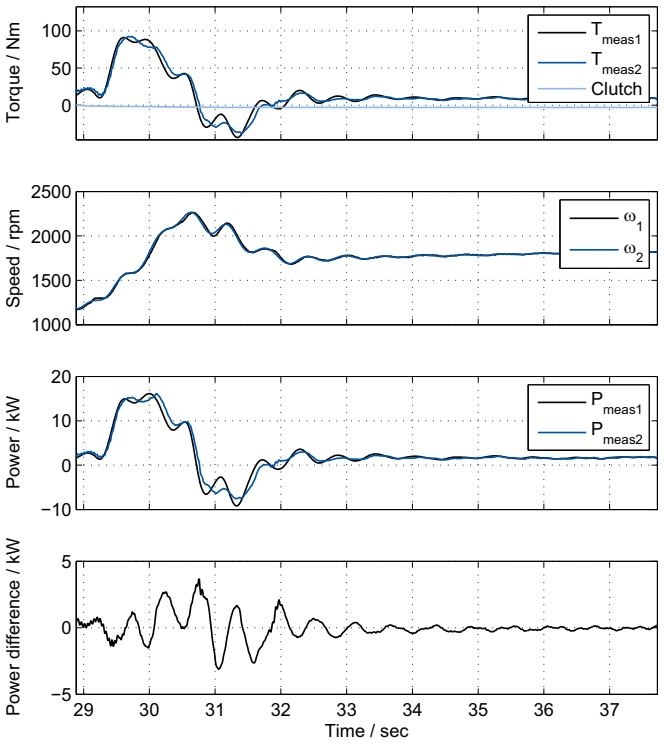

Fig. 15. Closed-clutch phase.

The technical data of the ICE are specified in Table 6. The control input is defined by the automatic driver and transmitted via the EtherCAT network to the engine TOM. The second test object is a manual transmission with an automated shift lever and clutch actuation directly controlled by the transmission TOM.

The VSA logic is implemented by two electric motors, whose parameters are specified in Table 7. The PID controllers used are parametrized for the closed-clutch situation in gears 1–5 according to the procedure described in Section 2.2. For detection of the open-clutch situation, the clutch actuator feedback signal is considered. In an open-clutch situation, the electrical load machine of the combustion engine is set to zero torque and the transmission electrical motor is operated in speed control to follow the engine speed.

To provide an objective and realistic investigation of the virtual shaft performance, a European driving cycle (ECE15) (Barlow, Latham, McCrae, & Boulter, 2009) was executed. The cycle consists of three positive velocity phases and is described in Fig. 13.

The blue line shows the real driven velocity and the red line shows the ECE constraints. Because the goal of the experiment is the evaluation of the VSA, high fluctuations in torque and speed were desired. Therefore, low-quality shifts and temporary validation of the speed limits are not only accepted but beneficial.

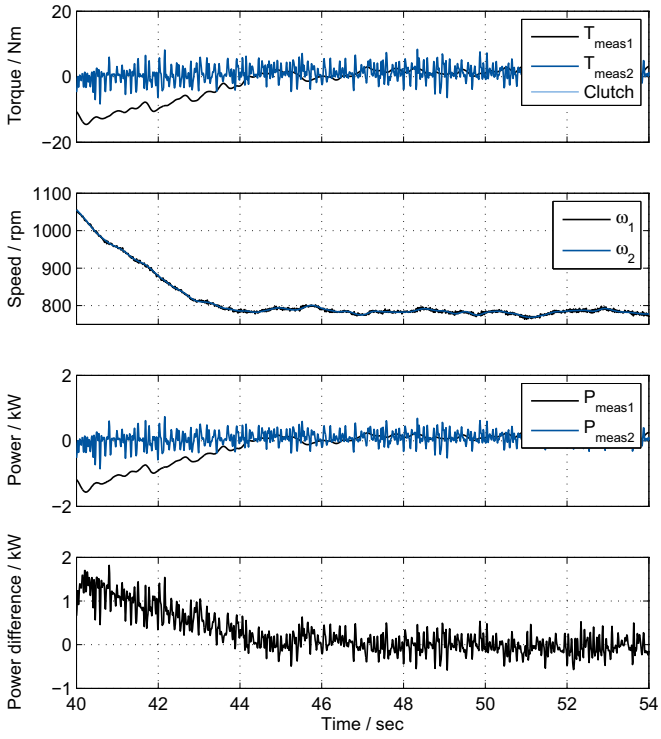

Fig. 16. Open-clutch phase.

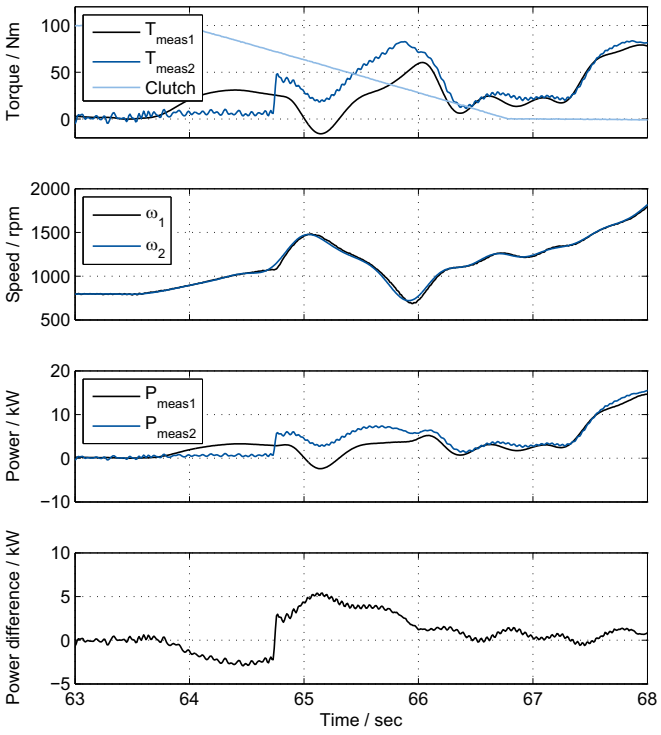

Fig. 17. Transition between open and closed clutch.

4. Measurement analysis

An evaluation of the VSA can be done by comparing speed and torque profiles in both test benches. A complete overview of the resulting speed and torque of both test benches is plotted in Fig. 14. The clutch actuator signal is scaled in the range of 0 (closed) to 100 (open). Because of the absence of a dedicated reference value, the percentage control error cannot be described as absolute control error related to the reference. Instead, the absolute difference of the mechanical power is considered.

The ECE cycle demonstrates good synchronization of both sides of the VSA from a macroscopic viewpoint. A significant control error appears around 150 s. This deviation is caused by the restriction of the maximum output torque of the transmission input electrical motor. Hence, no conclusion about the control performance in this time range is possible, but subsequently the control error is minimized again.

Because of significant differences in system behavior, the states in which the clutch is closed and open and the transition phase will be analyzed separately.

4.1. Engaged-gear situation

A common use case of the VSA is characterized by a closed clutch with an engaged gear and an equivalent inertia J_{EQ} that is dominated by the vehicle inertia. This situation occurs during driving with the exception of a slipping clutch at initial vehicle motion and during gear changes. Fig. 15 shows an excerpt of the ECE test. The clutch is closed (position = 0%) and the VSA is active. The automated driver is following the vehicle speed profile, which leads to common torque and speed profiles of the combustion engine output and the transmission input, respectively. The engaged gear is used for the selection of the appropriate set of PID gains. The VSA ensures that both signals converge without usage of any a priori knowledge of the drive cycle.

The system reactions to transient torque changes of the ICE show a lag of the transmission input torque owing to the inevitable communication latencies. The torque phase error leads to oscillation of the power error of ≈ 2 Hz. At steady-state conditions, the power difference converges to zero.

The VSA shows excellent potential application for situations with constant boundary conditions, characterized by the equivalent inertia J_{EQ}. A proof of controller stability was given in the simulation and at the test bench setup when utilizing strictly deterministic EtherCAT communication with constant latency.

4.2. Open-clutch situation

Based on preliminary simulations, the VSA logic has to be changed in situations of very low equivalent inertia J_{EQ} in systems with communication latencies. As described in Section 2.4, the torque synchronization is deactivated to avoid unstable operation and component damage. The torque controller of the transmission input electrical motor is deactivated; instead, the speed of the combustion engine ω_1 is the new set point.

This situation occurs at engine idle and during shifting. When the gear change process is terminated, the clutch is closed and the VSA is reactivated.

The measurement of an open-clutch situation is shown in Fig. 16 and indicates very good synchronization of the speed signals at transient ramp-down and at steady-state engine idling. The maximum speed error is <1% and its mean value is $\approx 0.1\%$.

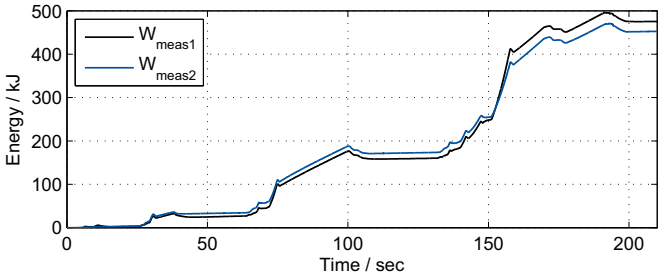

Fig. 18. Energy effort.

In contrast to the expected data, the measured torque on the ICE side, T_{meas1}, is not equal to zero during ramp-down. This is because of the additional electrical motor inertia that is added to the system in comparison to the reference layout. The implicit inertia compensation is not effective when the torque synchronization controller is deactivated. Apparently, this torque error is only effective on the ICE side, as the transmission input is speed controlled and the shaft inertia J_{s2} is very small. Obviously, the resulting torque synchronization error directly effects the energy balance of the system.

Changing the control logic in an open-clutch situation guarantees system stability. However, consistency of the transmitted torque and power is no longer given. In addition, the system speed differs from that of the reference system owing to the additional inertia. Active compensation of the electrical motor inertia is required to achieve good congruence with a mechanically coupled system.

4.3. Transition state

The transient phase between both VSA states is of particular relevance because the system behavior changes drastically. The clutch ensures a smooth blending on the mechanical side, whereas the controller has two discrete states. The clutch signal is compared to a threshold for determination of the preferred VSA strategy. Fig. 17 shows a vehicle launching with a continuously closing slipping clutch. Simultaneously, the ICE torque is increased. Because the system is in a sole speed control mode and no torque feedback is active, the torque increase is only visible at the engine side and the power error shows a value of ≈ -3 kW. At $t=64.8$ s, the VSA is switched to active torque control and after a transient phase of ≈ 1.5 s torque and speed synchronization are reestablished.

The equivalent inertia J_{EQ} cannot easily be calculated in a slipping-clutch situation. Fig. 17 shows clearly that intermediate states with a slipping clutch cannot be covered by discrete VSA controller parameterization. The VSA approach has to be expanded for sufficient control quality during transient conditions.

4.4. Energy balance

From a superordinate or fuel effort viewpoint energy consumption of both systems is more important than the exact synchronization of torque and speed. Therefore, the energy throughput of both test benches is subsequently analyzed. The energies of the two systems are plotted in Fig. 18 and must be even for a suitable substitution of the real shaft.

The diagram shows the converted energy in the entire test cycle. The mean energy error is 4.92% at the end of the test. Two main reasons for this deviation can be identified. First, the torque feedback loop deactivation in an open-clutch state has a negative impact. The additional inertia of the electric machine influences the energy balance of the VSA (Fig. 16). Another reason for the discrepancy is the limitation of the transmission input electrical motor, as shown in Fig. 14. Apparently, the constraint leads to a difference in transmitted power and deterioration of the energy balance. This result in Fig. 18 shows that the VSA in the current setup is suitable for initial fuel consumption estimations. How to improve the energy balance should be studied in further work. Because the transient torque and speed profiles show significant differences, emissions that depend on transient operation have a lower accuracy. For better accuracy of emission measurements, particularly the transient behavior accuracy has to be enhanced.

5. Conclusions

In this study, the substitution of a physical shaft connection between two powertrain components was evaluated. The mechanical shaft was mathematically described. Two electrical motors were used to emulate the respective ends of a spatially distributed powertrain. The VSA was applied to a conventional powertrain between a combustion engine and a transmission. A cascaded control structure, derived from force feedback applications, was chosen for torque and speed synchronization. The VSA consists of two PID controllers, whose parameterization depends on the system states: the clutch state and the engaged gear. This leads to the conclusion that the VSA requires knowledge about the system, in contrast to a real mechanical shaft. Simulations have been performed to study the effects of communication latencies. It was shown that the open-clutch scenario requires special handling to avoid unstable operation. The VSA was tested on a real automotive powertrain in a standard ECE drive cycle with an automated driver. For the closed-clutch phase good convergence was shown except for a phase shift with a frequency of 2 Hz. The open-clutch scenario has limits based on changing rotational speed. The additional inertia affects the system behavior and degrades the system accuracy. In particular, the transient behavior when the clutch is slipping poses significant challenges. Control accuracy by a VSA with discrete states is not sufficient. Nevertheless, the overall energy balance shows <1% difference and is suitable for powertrain layout. One possible option for optimizing the virtual shaft control deviation during gear change events is using a feed-forward lead-lag compensation of the external torque. This approach requires a direct measurement of the disturbance variables, e.g. the internal combustion engine torque derived from gas pressure of each cylinder.

Further work will focus on possible controller layout improvement by using system knowledge. As an example, the use of the current clutch capacity as an input for a gain scheduling controller is expected to enhance the transient behavior during shifting. Another approach that will be investigated in the future is to use adaptive parameters derived from observation of the clutch position. Furthermore, the effects of active inertia compensation during transient periods have to be analyzed in detail.

Acknowledgments

This work was partially performed as part of the graduate school 'GRK 1856 mobilEM – Integrated Energy Supply Modules for Roadbound E-Mobility', which is funded by the Deutsche Forschungsgemeinschaft (DFG).

This work was partially performed within the "Center for Mobile Propulsion", which is funded by the Deutsche Forschungsgemeinschaft (DFG).

References

Amberkar, S., Bolourchi, F., Demerly, J., & Millsap, S. *A control system methodology for steer by wire systems*. SAE technical paper, 2004. http://dx.doi.org/10.4271/2004-01-1106.

Anderson, R. G., Meyer, A. J., Valenzuela, M. A., & Lorenz, R. D. *Web machine coordinated motion control via electronic line-shafting*. IEEE paper 9031571. http://dx.doi.org/10.1109/28.903157.

Andert, J., Huth, T., Savelsberg, R., & Politsch, D. (2015). Testen von antriebssträngen mit der virtuellen welle. *ATZextra*, *20*(8), 30–35. http://dx.doi.org/10.1007/s35778-015-0044-7.

Andert, J., & Savelsberg, R. (2015). *Verfahren zum betreiben einer prüfanordnung Sowie prüfanordnung.*

Barlow, T. J., Latham, S., McCrae, I. S., & Boulter, P. G. (2009). *A reference book of driving cycles for use in the measurement of road vehicle emissions.* IHS Inc., Berkshire, United Kingdom.

Bertoluzzo, M., Buja, G., & Menis, R. (2007). Control schemes for steer-by-wire systems. *IEEE Industrial Electronics Magazine*, *1*(1), 20–27. http://dx.doi.org/10.1109/MIE.2007.357171.

Boksenbom, A. S., Hood, R. *General algebraic method applied to control analysis of complex engine types*. Report NCA-TR-980. National Advisory Committee for Aeronautics, 1950.

Cena, G., Bertolotti, I. C., Scanzio, S., Valenzano, A., & Zunino, C. (2012). Evaluation of ethercat distributed clock performance. *IEEE Transactions on Industrial Informatics*, *8*(1), 20–29. http://dx.doi.org/10.1109/TII.2011.2172434.

Dodds, C J., & Plummer, A. R. (2001). *Laboratory road simulation for full vehicle testing: A review*. SAE technical paper. http://dx.doi.org/10.4271/2001-26-0047.

Föllinger, O., & Konigorski, U. (2013). *Regelungstechnik: Einführung in die Methoden und ihre Anwendung* (11th ed.). Berlin [u.a.]: VDE-Verl.

Kenned, Jack J., & Patil, V. R. Control strategy and simulation in steer by wire system. *International Journal of Scientific Engineering and Technology*, *3* (7), 2014, 994–997.

List, H. O., & Schoeggl, P. *Objective evaluation of vehicle driveability*. SAE technical paper 980204, 1998. http://dx.doi.org/10.4271/980204.

Liu, G. F., Li, S. L., & Zhang, L. (2012). The synchronization control of the hydraulic press brake based on the virtual shaft control algorithm. *Advanced Materials Research*, *383–390*, 574–579. http://dx.doi.org/10.4028/www.scientific.net/AMR.383-390.574.

Lorenz, R. D., & Schmidt, P. B. *Synchronized motion control for process automation*. IEEE 96869, 1989. http://dx.doi.org/10.1109/IAS.1989.96869.

Luyben, W. L. (1970). Distillation decoupling. *AIChE Journal*, *16*(2), 198–203. http://dx.doi.org/10.1002/aic.690160209.

Normey-Rico, J. E., & Camacho, E. F. (2007). Control of dead-time processes. In *Advanced textbooks in control and signal processing*. Berlin and London: Springer.

Pérez-Pinal, F. J., Nuñez, C., Álvarez, R., Cervantes, I. *Comparison of multi-motor synchronization techniques*. IEEE 1431832 2, 2004. http://dx.doi.org/10.1109/IECON.2004.1431832.

Payette, K. (1998). *The virtual shaft control algorithm for synchronized motion control*. IEEE 688409 5. http://dx.doi.org/10.1109/ACC.1998.688409.

Payette, K. (1999). *Synchronized motion control with the virtual shaft control algorithm and acceleration feedback*. IEEE 786296 3. http://dx.doi.org/10.1109/ACC.1999.786296.

Pelkmans, L., & Debal, P. (2006). Comparison of on-road emissions with emissions measured on chassis dynamometer test cycles. *Transportation Research Part D: Transport and Environment*, *11*(4), 233–241. http://dx.doi.org/10.1016/j.trd.2006.04.001.

Schröder, D. (2009). *Elektrische Antriebe – Regelung von Antriebssystemen* (3rd ed.). Berlin, Heidelberg: Springer.

Sciuto, M., & Hellmund, R. (2001). "road to rig"– simulationskonzept an powertrain-prüfständen in der getriebeerprobung. *Atz – Automobiltechnische Zeitschrift*, *103* (4), 298–307. http://dx.doi.org/10.1007/BF03224372.

Sun, D. (2003). Position synchronization of multiple motion axes with adaptive coupling control. *Automatica*, *39*(6), 997–1005. http://dx.doi.org/10.1016/S0005-1098(03)00037-2.

Tomizuka, M., Hu, J.-S., Chiu, T.-C., & Kamano, T. (1992). Synchronization of two motion control axes under adaptive feedforward control. *Journal of Dynamic Systems Measurement, and Control*, *114*(2), 196–203. http://dx.doi.org/10.1115/1.2896515.

Wang, H., Kong, H., Man, Z., Tuan, D. M., Cao, Z., & Shen, W. (2014). Sliding mode control for steer-by-wire systems with ac motors in road vehicles. *IEEE Transactions on Industrial Electronics*, *61*(3), 1596–1611. http://dx.doi.org/10.1109/TIE.2013.2258296.